Stony Brook University

Investigation of Facet Joint Capsule Biomechanics of the Lumbar Spine: A Finite Element Study

By

Denis Evangelista

To

The Graduate School

In Partial fulfillment of the

Requirements

For the Degree of

Master of Science

In

Biomedical Engineering

Stony Brook University

May 2011

Stony Brook University

The Graduate School

Denis Charles Evangelista

We, the committee for the above candidate for the

Master of Science degree,

Hereby recommend acceptance of this thesis

Yi-Xian Qin, Doctor of Philosophy

Advisor, Professor, Department of Biomedical Engineering

Wei Lin, Doctor of Philosophy

Committee Chairman, Assist. Professor, Department of Biomedical Engineering

Yu Zhou, Doctor of Philosophy

Committee Member, Assist. Professor, Department of Mechanical Engineering

This thesis is accepted by the Graduate School

Lawrence Martin

Dean of Graduate School

Abstract

Investigation of Facet Joint Capsule Biomechanics of the Lumbar Spine: A Finite Element Study

By

Denis Charles Evangelista

Master of Science

In

Biomedical Engineering

Stony Brook University

2011

Low back pain is one of the most costly ailments in the world today. A key biological structure studied in the research of low back pain is the facet joint. The facet joint is thought to both play a role in the causation of low back pain through its response to noxious loading and in its relief through beneficial loading caused by spine manipulation. The purpose of these studies is to use a computational model to predict the biomechanical response of the facet joints to various loading parameters. This was accomplished using a linear 3D Finite Element model of the T12-S1 vertebrae of the spine with detailed facet geometry. The model was validated against a cadaver model under simulated chiropractic spine manipulation. The model was then modified and utilized to observe the effects of microgravity of the facet joints and predicted that the

facets do not play a role in the cause of back pain among astronauts due to exposure to microgravity environments. Finally, the model was modified to have degenerated discs at the L5S1, L4L5, and L3L4 vertebral gaps and was used to show that degenerated discs affect the stresses and strains on the facets in adjacent intervertebral gaps.

Contents

List of Figures

List of Tables

Acknowledgements

I would like to thanks my advisor Dr. Yi-Xian Qin for his consistent support and guidance over the past three years and giving me the motivation to succeed, even when I felt that I could not. Your guidance helped ease me into learning Finite Element Theory and introducing me to ABAQUS and its labyrinthine depths. I will always appreciate your patience, encouragement, and guidance.

I would like to thank the chairman of my committee Dr. Wei Lin for his external perspective on my model, technical help with MATLAB, and aid in setting up the new hardware that allowed me to run such a complex model. I would also like to thank my external committee member Dr. Yu Zhou for being able to be available on such short notice.

Special thanks go out to my partners at Palmer College and the University of Toledo. Dr. Vijay Goel and Vivek Palepu of the University of Toledo provided the base model of the spine used in this study. Dr. Ram Gudavalli and Ting Xia of Palmer College performed the cadaver tests that provided the data used to validate the model, with help from Allyson Ianuzzi who programmed the data collection algorithm.

I'd also like to thank my lab mates Suzanne Ferrari, Fred Serra-Hsu, Bo Chen, Jiandong Yu, Kevin Oon and Lianjun Lin. I'd like to thank Suzanne, without whom I'd not have the first idea as to how to work with ABAQUS. Thanks for your technical help, for helping me realize my strengths and limitations, and for helping me keep an eye on the prize. I'd like to thank Fred for all his help with MATLAB and any computational

snafus I got myself into. Congratulations on your engagement and good luck in the home stretch for your dissertation. I'd like to thank Bo Chen, Jiandong Yu, and Kevin Oon for being on the dream team in the summer of 2010 all of whom helped convert the facets into their new form. I couldn't have done it without all of your knowhow in Catia, SolidWorks, and Hypermesh, and I couldn't believe how quickly we were able to accomplish it.

Last but certainly not least I'd like to thank my partner in crime Lianjun Lin. We've been through a lot since we both came into the program in August of 2008, from the serious stuff like critiquing each other's papers, dealing with class, bouncing ideas, and making our power points, to the fun stuff like you teaching me about Association Football and me teaching you about American Football. Best of luck in whatever you decide to do bro.

1. Background

1.1 Low Back Pain Definition and Epidemiology

Low back pain is one of the most significant health problems in the world. It affects 25%-60% of Americans annually based on the definition used, [3] and 60%-80% of Americans are affected by low back pain in their lifetime [4]. 15%-20% of the adult population is stricken with low back pain at any given time [5], and low back pain is the second most common reason for visits to a physician behind headaches [6]. The cost of back pain in the United States in 1990 was estimated to be between $50 billion and $100 billion between both medical costs and lost productivity, with 194 million work days lost due to the ailment [7].

Low back pain (LBP) is defined as pain or discomfort in the region between the bottom of the ribcage and the coccyx, in the region of the lumbar section of the spine [8]. This may be accompanied by sciatica, which is pain that radiates from the back, most commonly to the legs [9]. There are two major classifications of LBP: acute and chronic. Acute LBP is back pain that lasts for less than 3 months in duration. Acute LBP usually goes away on its own and generally does not require any sort of intervention. Chronic LBP is back pain that lasts for more than 3 months or recurs within a 3 month time span after fading away. Chronic LBP often calls for intervention [8]. Most patients experience acute LBP; most cases of LBP are resolved in short order and 90% of individuals who miss work due to LBP return to work within 2 months time. Patients who experience chronic LBP have a poorer prognosis: only 50% of patients with

debilitating LBP that lasts for over 6 months return to work, with those experiencing pain for over 2 years having almost no chance of returning [9].

Back pain is also classified as specific or nonspecific. Specific back pain has an identifiable source, such as a collapsed vertebra or herniated IVD that has been found to be pressing against a nerve. Specific LBP can often be relieved by treating the source of the pain. Unfortunately specific back pain accounts for only 10% of all cases of back pain [9]. On the other hand nonspecific LBP has no identifiable source. Since there is no source to treat, treatment of nonspecific LBP is often restricted to symptom relief.

There are many risk factors for nonspecific LBP, though for many the reason why the factor contributes to LBP is unknown. Back pain is more common amongst the elderly due to loss of intervertebral disc height and osteoporosis of the vertebrae. Low strength of abdominal muscles and back muscles can cause the spinal column to be poorly supported. Smoking and obesity are other physiological factors that are associated with LBP. LBP has also been found to be associated with psychological factors such as stress, anxiety and depression [9].

1.2 Anatomy of the Spine

The spine is a column of bone and soft tissue that runs down the dorsal aspect of the human body designed to carry loads and protect the spinal cord. Most humans have 24 vertebrae that are separated into 3 major regions: cervical (C-1 through C-7), thoracic (T-1 through T-12) and lumbar (L-1 through L-5). Some humans have an extra vertebra in the thoracic region labeled T-13. Below the lumbar vertebrae are the sacrum and the coccyx, regions of fused vertebrae that connect the spine to the pelvis. The coccyx is the vestigial human remnant of the tailbone. Each region has a natural curvature known as primary curvature: the cervical and lumbar regions have natural kyphosis (convex curvature in the ventral direction) while the thoracic region has natural lordosis (concave curvature in the dorsal direction).

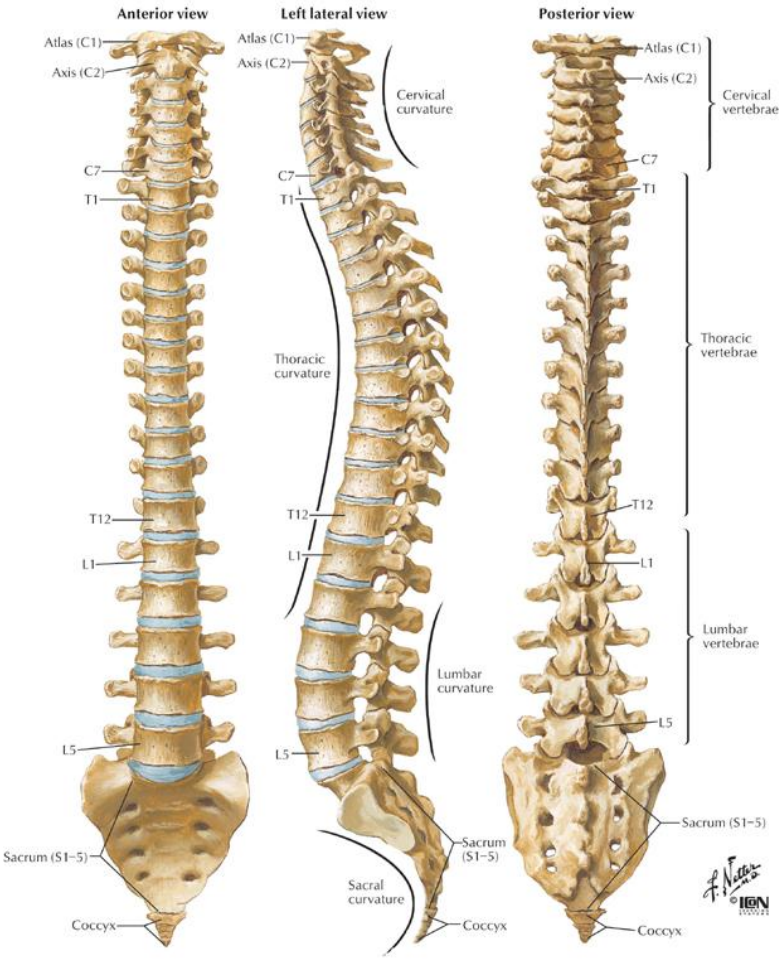

Figure 1 – Anatomy of the Spine. source: http://www.yland.com/Espanol/spine2d.asp

The vertebrae themselves have two sections: the main body

which borders the intervertebral discs and the neural arch which forms the spinal canal. The main bodies are connected to the intervertebral discs (IVDs) via the vertebral endplates, the concave superior and inferior surfaces of the vertebral body. The neural arch encircles the spinal cord and has 3 protrusions known as processes: the spinous process which runs in the ventral-dorsal direction and the transverse processes which run laterally, 90^{o} with respect to the spinous process. The spinous process is the bony part that can be felt through the skin on the back and is the structure most commonly manipulated in a spine manipulation. The neural arch also has four facet joints on it, two each on the superior and inferior sides. The facets of two facets join to form synovial joints known as zygapophyseal joints that serve as secondary connections between adjacent vertebrae. While the IVDs contribute the most to support the body and bear loads while the facet joints' primary function is to provide stability to the spine. When an IVD can no longer bear loads as it is supposed to, the load is transferred to the facets which can cause back pain, as will be described later.

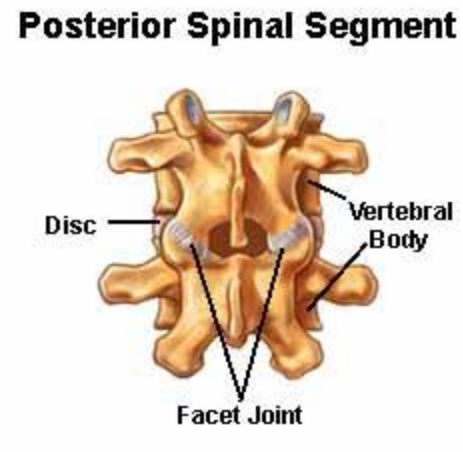

Figure 2 – Anatomy of the Facet joints. source: spineuniverse.com

The IVD itself is made up of two components: the fibrous annulus fibrosis, and the fluid nucleus pulposus. The annulus is a series of concentric lamella that contains fibers at various angles. It surrounds the nucleus, which is high in proteoglycan content. The PGs are hydrophilic and can attract and hold large amounts of water. In fact, most of the mass of the nucleus is water, ranging from 70%-90%. Water cycles into and out

of the nucleus over the course of a normal day. The water flows into it at night when in a supine position and forced out due to pressure on the nucleus due to gravity when upright in a standing position. Overall water content also decreases with age. Age-related water loss in the nucleus is the cause of degenerated discs, which will be discussed later.

2. Confirmation of the Linear Model of the T12-S1 spine

2.1 Introduction

2.1.1 Treatment of Low Back Pain

Numerous treatments are used to provide relief for low back pain. Due to the often idiopathic nature of LBP, doctors and chiropractors must treat the symptoms rather than the cause. Surgical procedures to alleviate low back pain are only undertaken if a potential specific cause for the LBP is identified, like a herniated disc pressing on a nerve or a vertebral fracture, and only if the LBP is debilitating to the point of interfering regularly with normal functions. Herniated discs can be replaced with synthetic discs or removed altogether and filled in with a solid material to fuse the vertebrae together [10].

Newer therapies focus on destroying the nerves causing the pain instead of causing radical biological change. For pain from nerves on the IVD, Intradiscal Electrothermal Therapy (IDET) inserts an electrode into the IVD which acts as a resistor to electric current, heating up and killing the nerves with heat [11]. Nerve death via heat has also shown promise in animal models via ultrasound, which has been shown to have advantages over IDET including directional heating and greater thermal penetration. Back pain from nerves innervating the facet joint can get relief through radiofrequency ablation, which destroys the nerves innervating the facet joints via heat death [12].

The most conservative therapies include exercise regimens for the muscles surrounding the spine, acupuncture, NSAID pain relievers, and spine manipulation. The abdominal muscles and those around the trunk of the spine apply loads to the spine that aid in the spine's stability. Strengthening these muscles has been shown to improve spine stability which in turn reduces low back pain. These exercises are often organized into clinical programs known as back schools, which also teach spine anatomy and proper posture. Back schools emphasize exercises that strengthen the spine as well as the how to sit, lift, and lie down in ways that prevent unnecessary strain on the body [13].

Acupuncture is an alternative medicine method that originated in China which involves insertion of metal needles into the skin at specific points. It has been found that the needles stimulate certain neurons that cause systemic opioid release and local adenosine release, but there is insufficient evidence to create a unified theory on the method of pain relief. It has application in low back pain relief as a complementary or alternative practice and is applied via 5 major insertion points known as medians for LBP relief [14]. Non-steroidal anti-inflammatory drugs (NSAIDs) are a class of pain relievers that include aspirin and similar compounds as well as COX-2 inhibitors. They are indicated for general systemic pain relief, including LBP, by way of anti-inflammatory, analgesic, and antipyretic effects [6].

2.1.2 Spine Manipulation

Spine Manipulation (SM) is a type of back pain management that is accomplished by applying a physical force to the spine [15]. SM has been practiced for more than 2000 years [16] and in modern times is most commonly performed by chiropractors [17]. The most common form on SM is high-velocity low-amplitude (HVLA) thrust manipulation, in which high velocity thrusts are applied to synovial joints of the spine. The goal is to create an audible crack, which signifies a successful manipulation [18].

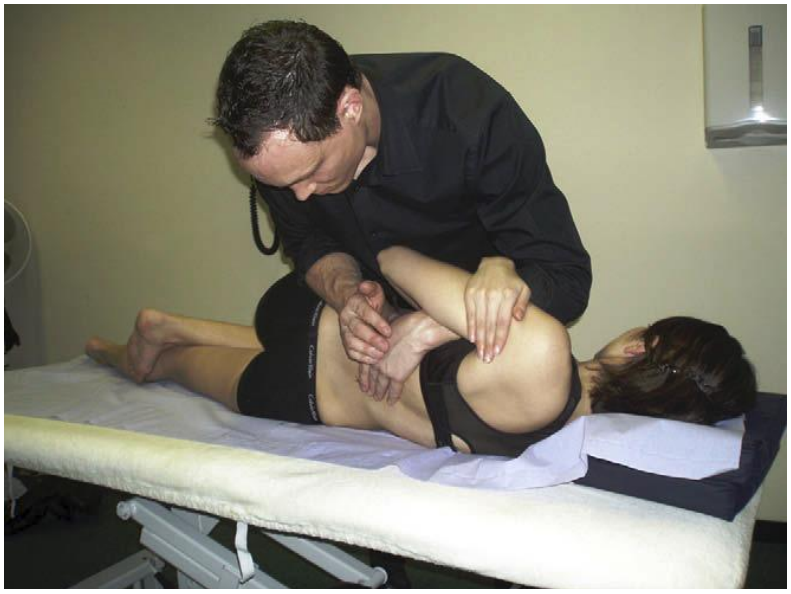

Figure 3 – An example of Spine Manipulation source: [1]

SM is performed via dynamic thrusts to a specific vertebra. HVLA thrusts are performed using a quick thrust on the vertebral processes with a short lever arm. Quantitative classification of HVLA SM has revealed that it consists of a pre-load force of 20-180N followed by a larger impulse force of 220-550N over the course of 200-420ms, with the smaller forces corresponding to cervical manipulations and the larger corresponding to lumbar manipulations [19].

Spine Manipulation has been clinically shown to relieve chronic low back pain. A review of various clinical studies showed that while SM was not shown to be effective at

relief of acute LBP, 5 of 8 studies examining SM for use in chronic LBP relief found it to be superior to one or more alternative treatments, among them bed rest, analgesics, massage, sham manipulations, back schools, and bed rest. Some studies have shown negative outcomes resulting from SM, suggesting that certain patients are poor fits for SM. Unfortunately, it is currently unknown what criteria make for a good or bad prospective patient for SM [20].

There have been numerous theories as to the cause of the cracking sound as well as the mechanism by which LBP is relieved. Originally it was thought that SM realigned joints that were out of position, much in the same way that fractured bones and dislocated joints are set and realigned [2]. It was also thought that the manipulation would set a displaced IVD back into place, although SM has shown to have little if any effect on forcing herniated discs back into the intervertebral space. Recent studies have shown that a displaced nucleus of the IVD could be moved back into place via manual manipulation, but this would be a low velocity manipulation and is unrelated to the cracking sound that occurs in SM [21]. In addition, the crack being caused by movement of the IVD would not explain why other joints in the body would cause the cracking sound. The cracking sound is caused by cavitation in a synovial joint; in the

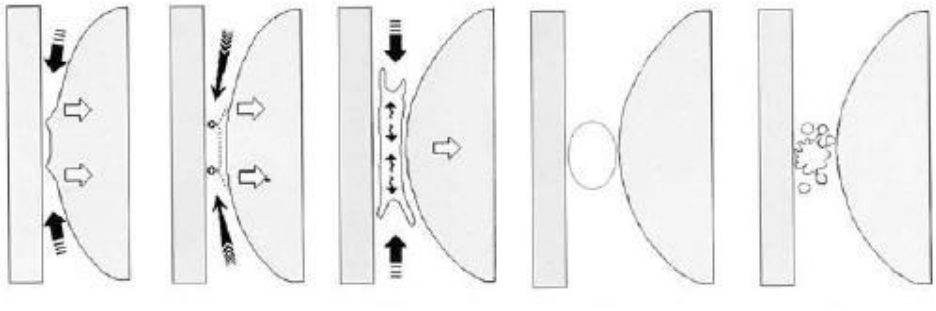

Figure 4 – Mechanism of cavitation of a synovial joint. source:[2]

case of SM, the cavitation of the Zygapophysial joint, also known as the facet joint. This cracking phenomenon has been used to signify a successful manipulation. There are 3 major theories as to how this is achieved. The first is a direct theory that the separation of the facets releases fibro-adipose meniscoids (cartilage discs at a joint) that have previously been observed to be present in facet joints [22]. These meniscoids are innervated and their entrapment in the joint sets off the type III and type IV nocireceptors in them causing the sensation of pain [23]. The SM creates a gap in the facet joints that would allow the meniscoid to return to its normal position in the joint, thus alleviating the pressure on the innervated meniscoid and reducing pain [24]. According to this theory, the cracking phenomenon, while signifying a successful manipulation, in simply a side effect of the gap being created in the joint. However, it is thought that this theory is only true for the relief of LBP due to “acute joint lock,” a pathology where it has been observed that meniscoid entrapment occurs. The theory fails to explain the other nonmechanical effects that have been observed in SM.

The second theory is based upon the viscoelastic nature of soft tissue in human physiology, applied in this case to the facet joint capsules. Viscoelasticity is a material property where the strain is dependent on the rate of loading of the applied stress. The synovial fluid in the facet joint has such properties, and as such absorbs a lot of the energy of the normally fast impulses of SM. [2] Thus when an impulse is applied, cavitation occurs at which point the resistance to the impulse drops precipitously. If the force imparted on the spine exceeds this force threshold to cause cavitation, found to be around 400 Newtons for the lumbar spine, then certain neuropeptides are released as a result. It has been shown that this phenomenon only occurs if cavitation occurs, as well

as only occurs in the facet joints, so the effect that is resultant appears to be dependent on the unique physiology of the facet joint capsule. The fact that Group III and Group IV afferent neurons have been found to innervate the FJC supports this theory[25]. This study is based on the assumption that this theory is the correct one as there is the most evidence in the literature that the pain relief caused by SM is neurological in nature.

The third theory is based on the thought that after the facet joint is pushed past the viscoelastic barrier, the joint is allowed greater mobility until the air bubble in the joint reforms. [18] After a cavitation event, the air in the joint is dispersed throughout the joint until it reforms into a bubble after approximately 20 minutes. During this time the joint cannot be cracked again, as its viscoelastic nature does not occur due to the fact that the air bubble is the cause of the viscoelasticity [26]. This allows the joint to move more freely, resulting in an increased range of motion. It is thought that this allows intra-articular adhesions in the joint to be released [2]. However, there are no correlations between increased mobility alone causing a relief of LBP [27].

2.2 Hypothesis

This study will attempt to create a linear finite element model of the T-12 to S-1 region of the spine that accurately models the real physiology of the region. Regions of interest are the facet joints, which have been shown to be a critical component in the relief of LBP from SM. The hypothesis of this study is the facet joint capsule can be accurately represented with in a Finite Element model with linear facet joint material

properties. The specific aim of this study is to construct a Finite Element model of the spine with detailed linear facet membranes and validate the model using data obtained from simulated SM on a cadaver model.

2.3 Methods

2.3.1 Model Development

The model went through numerous iterations. The first utilized a pre-existing facet joint capsule mesh for the L3L4 and L4L5 gap from a previous model. Using MATLAB programming, the node coordinates of the mesh of the L3L4 joint were copied to the T12L1, L1L2, L2L3, and L5S1 FJCs. The copy algorithm took into account the varying size and positions of each FJC: the Toledo model was designed with the spine's natural curvature in mind. Hence, the MATLAB code used reference planes of nodes on the Toledo model's posterior bony segment to calculate adjustment

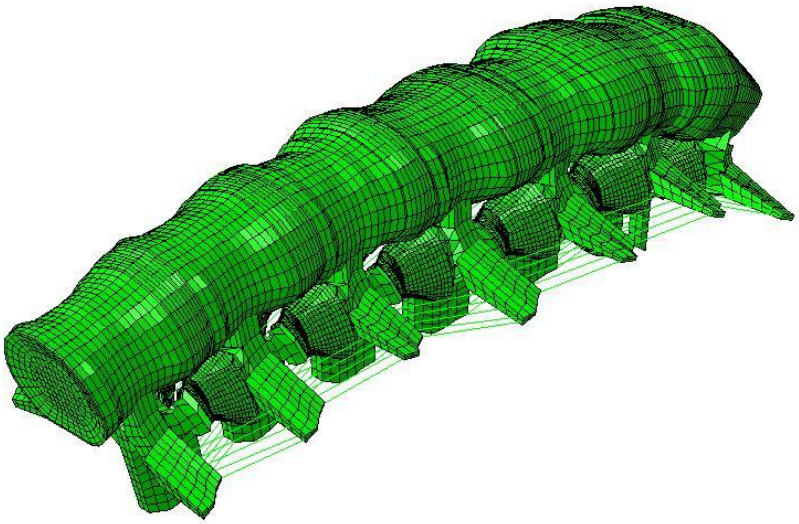

Figure 5 - Original FE model of the T12-S1 spine

factors for the FJC: translation in the y and z directions to account for position, angle in the y-z plane to account for rotation due to natural spine curvature, and scaling factors in the x, y, and z directions to account for differences in size between the vertebrae.

Problems with this model became apparent during initial validation runs when the facet membrane had astronomically high strain rates on it, with average strains often over 100% and sometimes reaching as high as 700%. Upon further investigation the facet membranes had poor mesh quality, with some elements arranged as triangular prisms rather than rectangular bricks. These elements were the cause of the high strains due to the abnormally large stress concentrations on the points where the membrane was pinched.

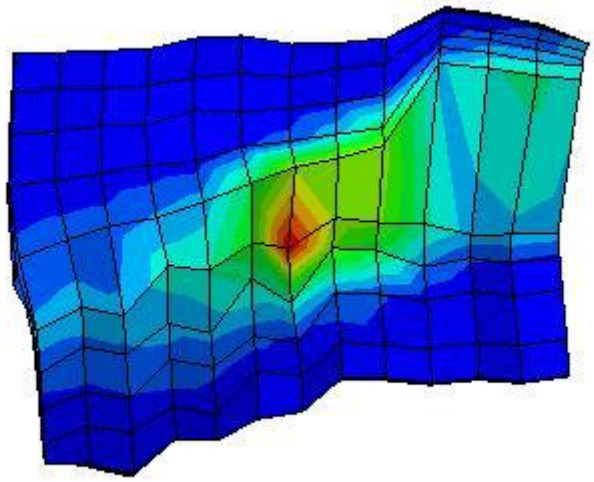

Figure 6 - Example of an abnormal stress concentration on the facet membrane of the original model

Attempts were made to modify the membrane to minimize these stress concentrations, but proved to be ineffective. Upon further investigation and consultation, it was deemed that the irregular geometry of the membrane and the facet were ill-suited to brick elements, and that the area should be remeshed using C3D4 tetrahedral elements. This would reduce stress concentrations and aid in overall mesh quality as tetrahedral elements can more easily conform to irregular shapes, reducing the number of distorted elements.

To remesh the facets and membrane, the geometry of the existing facet and membrane was deemed sufficient and that only the C3D8 brick-element based mesh had to be changed. To do this the model's geometry was tranferred into the Altair Hypermesh software suite in order to redo the mesh. However, this was more difficult than thought due to the fact that the mesh of the facet and membrane was not made in ABAQUS CAE but programmed manually in an input file. This made the mesh an orphan mesh when imported into both the CAE and Hypermesh environment, and as an orphan mesh it could only be modified, not deleted outright and replaced. An attempt was made to convert the brick elements into tetrahedral elements by bisecting them diagonally, but it did not produce any improvement.

Since conversion from an orphan mesh to a solid model was not possible, the model had to be rebuilt as a solid model that could be recognized by Hypermesh and ABAQUS. The model was rebuilt in SolidWorks CAD using the node coordinates of the bony facet from the ABAQUS .inp file. The node coordinates that formed the outline of each end plane of the L3-L4 bony facet were imported manually into SolidWorks. These coordinates were used as end-surfaces to create a loft feature that approximated the form of the existing facet in the model. Cut features were used to refine the solid model to make it more similar to the original geometry. Once the geometry was deemed to be a satisfactory facsimile to the original geometry of the orphan mesh, it was saved as a generic file type and transferred to the Catia CAD modeling program in order to produce the geometry for the facet membrane. An attempt was made to create the membrane in SolidWorks by following the contours of the facet and then bridging the gap between the two bony ends of the joint, but SolidWorks doesn't perform well

when creating irregular, non-geometric structures. All attempts at creating adjacent planes and lofting failed due to self-intersection. Catia is more powerful and better-suited to this application, and thus enabled us to successfully create the membranes in the intended manner.

After the membranes were added in Catia, the solid model was imported into Altair Hypermesh to be meshed with tetrahedral elements. Since one of goals of the remesh was to reduce distorted elements and increase the chances that the analyses on the model would converge, the mesh was made very fine. While the previous facet had 2988 total 8-node brick elements, the new facet had the new facet had the new facet had 260736 total 4-node tetrahedral elements. The membrane had a slightly finer mesh than the facet. Many secondary changes had to be made to the model due to the new facet joint. The joint had to be correctly positioned since it the nodes that were output by Hypermesh were in relativistic coordinates instead of absolute coordinates. The part was manipulated into its rightful place in ABAQUS CAE which, when exported into an .inp file, gave the translation factor, rotation axis and rotation angle that would manipulate the nodes into the correct position at the facet joint. MATLAB code was created that used the translation and rotation information to convert the node coordinates into their rightful spots. The facet was then reflected over the z plane in ABAQUS and copied from the L3L4 location to the other facet locations using a modified version of the MATLAB code that had done the same for the previous iteration of the model. Because of the much higher element density of the new facet, existing relations between the base model and the facet were insufficient. New TIE relationships had to be built between the new facets and the bridge elements that were

between the posterior bony elements and the old facet, and between the new facet and the elements representing the cartilage.

The model with the new facet had fewer distorted elements and had better convergence than the previous model. However, the model had a total of 3179790 elements which, coupled with the computationally expensive TIE commands, increased the processing time considerably. While the density of the new facet was deemed suitable for a detailed examination of a single facet, when copied to the other facets it resulted in a model with far too many elements for the computers systems available, resulting in models with runtimes greater than a week in duration.

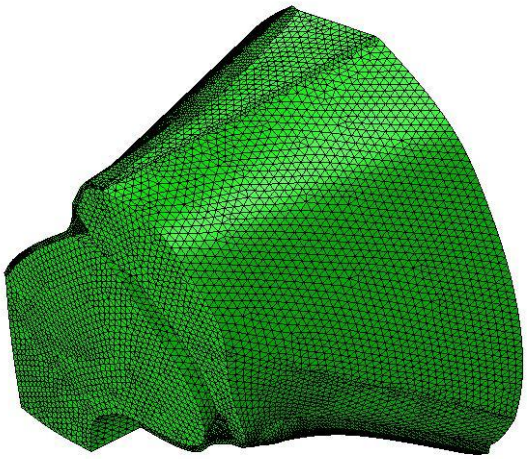

Figure 7 - Bony facet and facet membrane of the first revision of the FE model

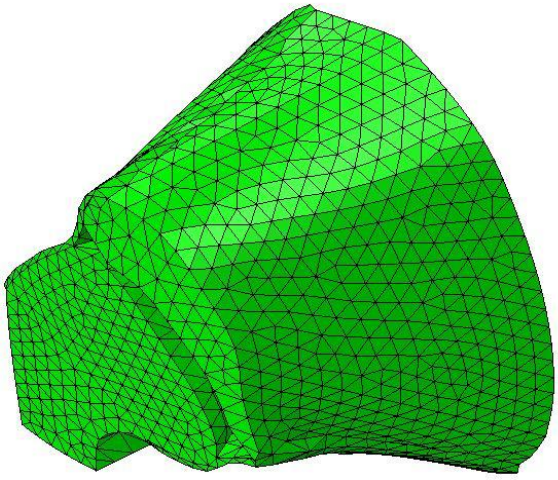

Figure 8 - Bony facet and facet membrane of the second and final revision of the FE model

Using the same geometry developed in SolidWorks and Catia, a new mesh was created in HyperMesh that still used tetrahedral elements, but a greatly reduced density. The new mesh had 14366 elements per facet. Again tie commands were used to attach the facet

to the bridge, but the lower number of nodes tied reduced the computational time. The cartilage elements were not tied on this iteration, but instead remodeled into tetrahedral elements and the nodes at the interface merged for a better connection. The resulting model had satisfactory performance in model stability, convergence, and processing time.

2.3.2 Model Validation

Validation of this model was performed by using simulated spine loading similar to that of spine manipulation. The original model with rough facets was validated against loading conditions of 10.5kN CCW rotation, followed by a 200N concentrated pre-load on the L5 posterior bony section, followed by a dynamic increase of the pre-load from 200N to 400N over 100ms. This is the same loading conditions used to validate the new model. Palmer College provided data using said loading conditions performed on a cadaver model of the spine. The model with detailed facets was validated against both the rough validated facet model and the cadaver model. Boundary conditions for the validation runs included fixing the bottom of the S1 vertebra in all steps is all 6 degrees of freedom, and fixing the top of the T12 vertebra in all 6 degrees of freedom from the second step (preload) on to the end of the analysis. The validation was run as a best fit match with the other sets of data, the independent variable changed being the material property of the facet membranes. The material properties tested were based on values previously used in the L3-L5 spine model: linear

elastic E=2.76, linear elastic E=5.08, and linear elastic E=8.08 with the poison's ratio on all being 0.3.

Global position data was compared between the model with detailed facets and the rough facet model from the University of Toledo. Facet strain data was compared between the model with detailed facets and the Palmer College cadaver model. The data obtained by Palmer College was obtained using a speckle pattern and special cameras, and thus only was able to detect 2D surface data. To reconcile the 2D surface data with the 3D data obtained from the facets in the computational model, the specific region and principle direction was found for the 9-node speckle pattern on the cadaver model. The matching region was found on the computational model, the strain data from that region taken, and then transformed using a rotation matrix derived from the Euler angles between the surface plane and the x-y plane. The data will be analyzed under the plane stress assumption as the membrane is thin and the data derived from the cadaver model is 2D surface data.

2.3 Results

The rotation matrix to convert the local coordinates into the x-y plane was created using a plane created from 3 points on the membrane of the computational model and finding the Euler angles between that plane and the x-y plane. This was done using the x-y-z convention for the Euler angles. Euler angles were found to be $\varphi = 74.2$, $\theta = 90$, and $\psi = 150$. Membrane strain data was only collected on the cadaver model on the right side of the L4-L5 membrane, which is where the points were selected from for comparison on the computational model. Matching regions on the computational model were found and organized into sub-regions equivalent to the size of the elements on the cadaver model: 1.667 mm in width by 3.333 mm in length. Below is the strain % error between the computational and cadaver models for each model, followed by graphs of the principal strains.

Strain % Error

		E=2.76	E=5.42	E=8.08
E1	x	-98.60%	-91.34%	-85.83%
	y	-83.85%	-83.79%	-84.88%
E2	x	330.25%	353.05%	309.02%
	y	99.28%	103.66%	83.54%
E3	x	-9.92%	77.91%	98.84%
	y	97.89%	146.76%	129.78%
E4	x	-0.44%	1.93%	-1.60%
	y	106.73%	121.92%	118.37%

Table 1 - Per element percent error of strain between the cadaver and computational model of the spine. The data compared was a section of the L4-L5 facet membrane.

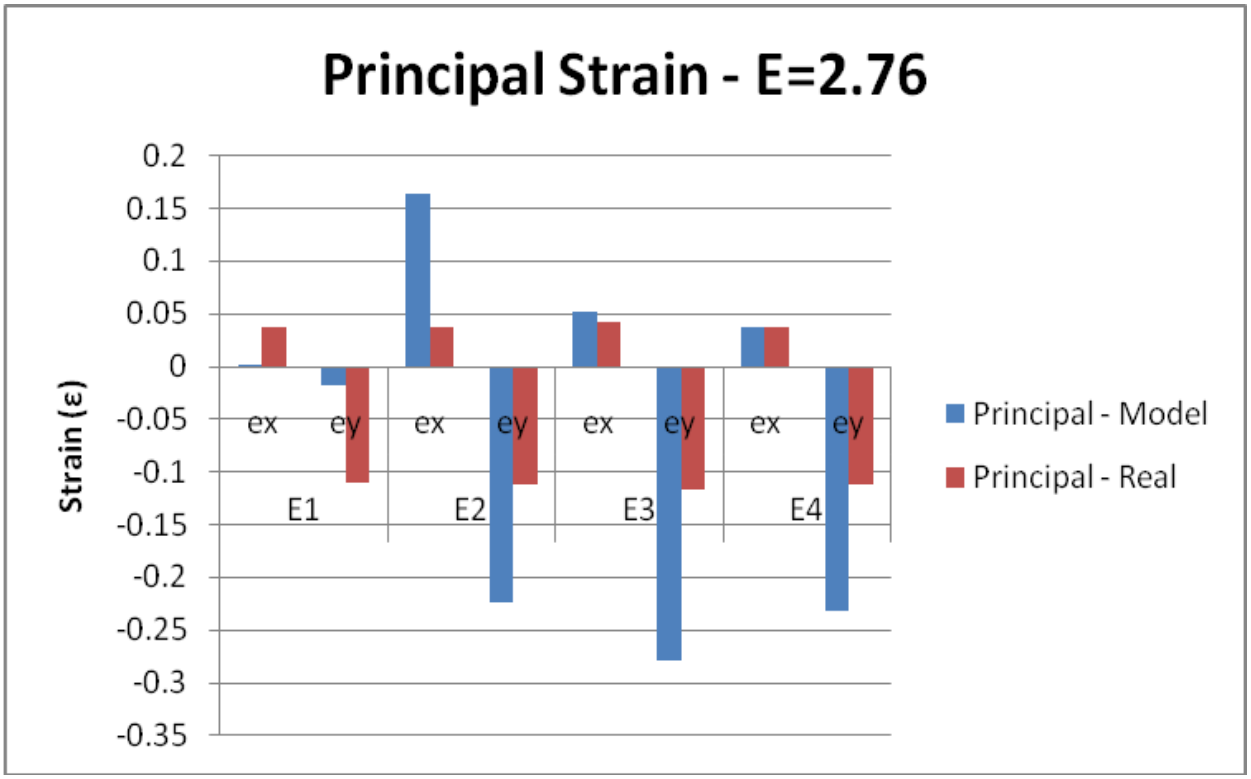

Figure 9 - Comparison of Principal Strain between the cadaver model and the computational model with membrane elastic modulus of E=2.76 MPa. E1, E2, E3, E4 refer to the 4-node 2D elements on the cadaver model which is compared to an analogous area on the computational model.

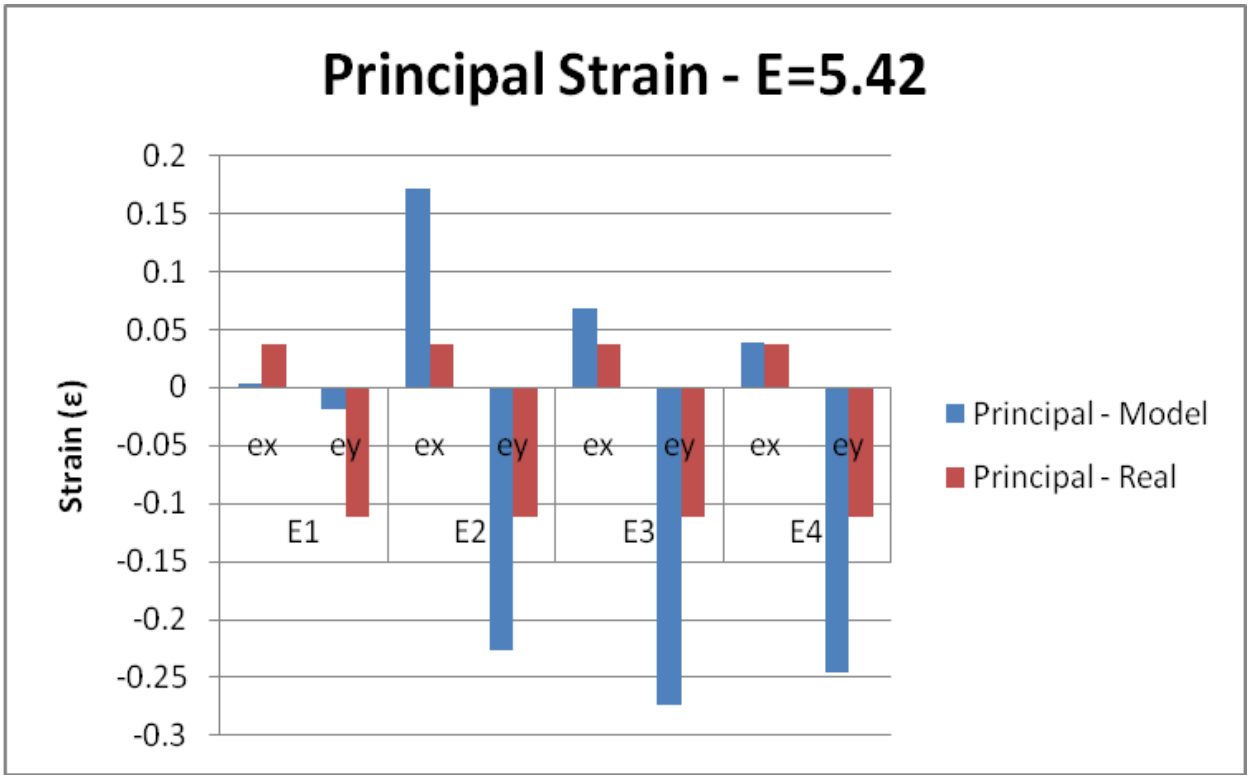

Figure 10 - Comparison of Principal Strain between the cadaver model and the computational model with membrane elastic modulus of E=5.42 MPa. E1, E2, E3, E4 refer to the 4-node 2D elements on the cadaver model which is compared to an analogous area on the computational model.

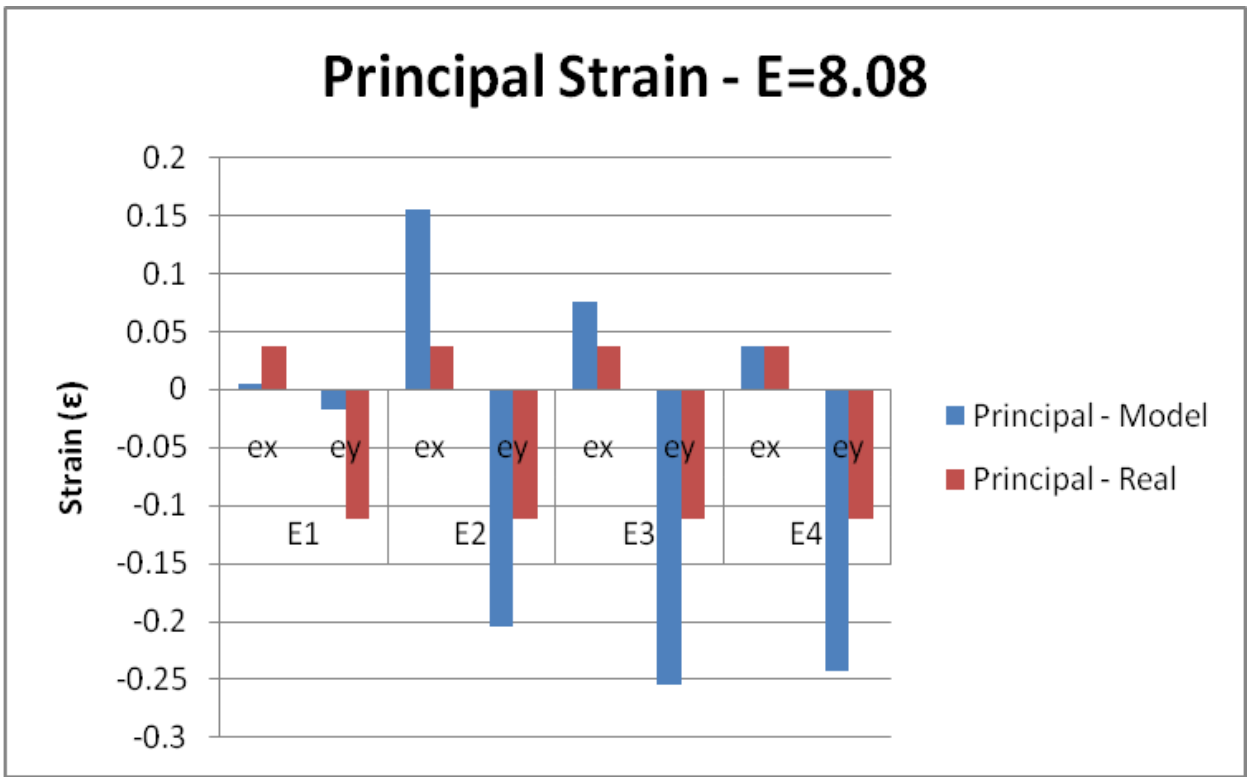

Figure 11 - Comparison of Principal Strain between the cadaver model and the computational model with membrane elastic modulus of E=8.08 MPa. E1, E2, E3, E4 refer to the 4-node 2D elements on the cadaver model which is compared to an analogous area on the computational model.

2.4 Discussion

The computational strains acquired by the model were often times very poor fits for the strains found in the cadaver model, regularly having percent errors near or exceeding 100%. In the membrane elastic modulus = 2.76 MPa case, the percent error between the computational and the cadaver model reached 330% for the element 2 principal strain in the x-direction. The E=5.42 and E=8.08 cases did not fare much better, both having percent error maximums at 353% and 309%, respectively, also at the element 2 x-direction principal strain. Many of the percent errors were close to one another showing that the models were close to one another in performance. The most prominent exception to this is the Element 3 x-direction principal strain, which had -9.92% error for E=2.76, 77.91% error for E=5.42, and 98.84% error for E=8.08. The value that is most consistent between the computational and the cadaver models is the Element 4 x-direction principal strain at -0.44% error for E=2.76, 1.93% error for E=5.42, and -1.60% for E=8.08. Since the disparity between the Element 3 principal strain is the only large difference between the models, the E=2.76 model therefore is the best fit since it has the closest value to the cadaver model for Element 3.

While the vast differences between the cadaver model and the computational models may write off the usability of a linear model for the detailed facets, there are some possible changes that can be made to the model to remove its limitations and help it be a better fit. First would be the fact that the facet membranes do not completely encapsulate the FJCs in the computational model. While considered an acceptable break from reality in previous models, it presents a few problems in the current model. Due to the fact that regions of the membrane are missing, a one-to-one

equivalency between the region of interest on the cadaver model and the computational model was not possible. In addition, certain movements could cause the missing regions to be vital to accurate, realistic responses due to the fact that the membrane takes on the compressive aspects of the synovial fluid in the FJC.

Another issue with the data is that the validation data is from the L4-L5 FJC on a single cadaver model. Due to normal human polymorphism the spine can have different physical and material properties based on genetics, health, and fitness. Having data collected from more samples would have given a more clear picture of the stresses and strains on the human body in general; as it stands with only one cadaver model this could be considered a case study. In addition, the only facet that cadaver data was collected from was the right L4-L5 facet. Being able to compare data from more FJC membranes at different parts of the spine would allow for a more complete view of how well the computational model fits the cadaver model. However, this brings up a logistical problem in that unless data could be collected from all FJCs simultaneously then more experimental variability is introduced into the data sets, as the data would be collected on separate runs on different cadaver spine samples.

Overall, the results show that while the computational data is not a great fit for the cadaver data, improvements can be made to both the cadaver model and the computational model to give a greater correlation between the data. It would be irresponsible to say that this study discounts the linear model, especially given the good correlation of element 3 and element 4 between the two models. Element 3 and

element 4 being closer to the site of loading in the computational model could be a reason for the better correlation of those data points as well.

3. The Facets' Role in LBP caused by Microgravity

3.1 Introduction

Back pain is a common complaint among astronauts during and following space flight. While not widely studied, a few studies have provided insight into the nature of the pain. Wing et al. examined 58 astronauts which found that 68% of astronauts experienced low back pain during spaceflight, with 28% describing the pain being moderate to severe in intensity. This pain was most often in the lumbar region and was most prominent in the early parts of the flight, during the first 6 days [28]. Mike Mullane corroborated this in his memoir Riding Rockets: the outrageous tales of a space shuttle astronaut, where he said that 5 of the 6 astronauts on flight STS 41-D experienced sever low back pain in the lumbar region during the 6 day mission. He also claimed that curling up in to the fetal position alleviated the pain [29].

Low back pain, while often having no discernable cause, can precede certain debilitating conditions, chief among them herniated intervertebral discs due to disc degeneration. There are concerns that the lumbar back pain experienced by astronauts could be the early signs of disc herniation, and that the discs may be degenerating as a result of spaceflight [30]. Indeed, a study revealed that astronauts have a higher rate of disc herniation than both the general population and Army aviators. The primary difference in spinal stress between aviators and astronauts is the experience of microgravity for the astronauts [28].

The vertebral column lengthens in microgravity to 4-6 centimeters [31], 3 times the normal daytime values in Earth gravity of 1.5-3 centimeters [32]. This is believed to be caused by the intervertebral discs swelling with fluid. The force of gravity and other forces such as the tension on the spine from the muscles that hold the spinal column in place force fluid out during normal diurnal activity while in the Earth's gravity. This counteracts the effect of natural fluid inflow that occurs due to ionic diffusion caused by the negatively charged proteoglycans present in the disc's nucleus pulposus [33-34]. While lying in a supine position as during bed rest, the spine is unloaded and fluid is allowed to flow in. Thus, during normal daily activity of supine slumber and daytime upright activity, the spine is loaded and unloaded in a manner that causes 25% of the total fluid to be imbibed and expelled in a 24 hour period [34].

In microgravity such gravitational forces are not present as well as the spinal muscles weakening due to disuse, so the fluid enters the IVDs and is not forced out causing the discs to swell past normal physiologic values. In addition, the swelling compromises the spine's natural curvature and causes it to become straighter. The mechanism by which LBP is resulted from these conditions is that expansion of the annulus fibrosis of the IVD past the normal physiological value of 3-4% activates Type IV mechanoreceptors, which will cause the sinovertebral nerves to transmit impulses and lead to the perception of low back pain [35]. It is because of this that it is believed that disc expansion beyond normal physiologic values is the cause of back pain in microgravity.

It is not believed that the facet joints contribute to LBP in microgravity due to the fact that curling into the fetal position relieves the LBP rather than aggravates it. However the facets may have a role in the relief of microgravity-induced LBP. As stated before, astronauts have claimed that curling into the fetal position provided short-term relief to LBP when in microgravity. This is believed to occur for two reasons. First, the fetal position shifts the majority of the spinal load to the discs from the normally more evenly shared load between the disc and the facet joints to the anterior portion of the IVD. This action compresses the IVDs and forces fluid out of them, restoring some semblance of normal physiology to the IVDs. Second, the fetal position stretches out the facet joints, activating Type I and II mechanoreceptors, which contribute to relief of LBP through the release of enkephalins, an opioid that neutralizes pain neurotransmitter Substance P [35].

There are several other concerns regarding IVDs in microgravity. The IVD itself lacks vasularization except for capillary flow in the outermost layers, so fluid flow is the primary way that the disc acquires nutrition. This loss of nutrition can cause damage to the IVDs [36]. The IVDs are also subject to Wolff's Law like bones. Wolff's Law states that a biological tissue remodels itself to become stronger with increased load on it. Without such a load, the biological structure atrophies. This is a concern with bone in both microgravity and extended bed rest, and the same has been found for the IVDs. With extended spaceflights, the likelihood of atrophy increases as the IVDs adapt to the environment of microgravity due to Wolff's Law. When the astronaut returns to a 1G environment, the degeneration of the disc from the flight could cause chronic LBP and disc herniation.

Efforts to reduce LBP through spinal while in spaceflight have been largely unsuccessful. Astronauts have been doing exercises on specialized equipment in order to keep their muscles strong and prevent bone hypertrophy, but the exercises have proven to be unable of providing enough intensity to prevent hypertrophy from occurring. The exercises include treadmill running where the astronaut is compressed to the treadmill by elastic bungee cords which compress the spine as a by-product, but the non-uniform compression causes discomfort on the contact points of the shoulder and pelvis. In addition, the compression itself is only 60-70% of that of normal gravitational compression [30]. It is worth noting that Russian cosmonauts do not have LBP complaints similar to astronauts, possibly due to the positive spinal traction provided by their “penguin suit” spacesuit which provides compression on the body. However, no studies have been carried out to examine this discrepancy [35]. Otherwise, astronauts are given painkillers to deal with the LBP, which alleviates the pain but does not do anything to prevent the deleterious effects that cause the pain [37].

3.2 Hypothesis

This study will use the validated, linear model of the lumbar spine from the T12 to S1 vertebrae to simulate the spine in microgravity. This will be accomplished via displacement controlled actions that will simulate spinal expansion from the intake of fluid into the IVDs. The hypothesis of this study is that the model of the spine in simulated microgravity will not show that the pain is caused by compression of the facet joints. The specific aim of this study will be to compare a T12-S1 spine model stretched

so that the IVDs expand by 10% to that of a similar spine model under gravitational loads. The secondary hypothesis is that the model in simulated microgravity when manipulated into the fetal tuck position will show facet separation concurrent with the strains needed for pain relief. The secondary specific aim of this study will be to compare the strains on the facet joint of a simulated T12-S1 spine in microgravity with that of a spine in microgravity that has been displaced in a manner similar to fetal position curling.

3.3 Methods

The base validated linear model of T-12 to S-1 with detailed facets from specific aim 1 will be used, and will include the best fit linear material property that was determined for the facet joint membrane. There will be three different versions of the model that will change boundary and loading conditions: the first will be a control model having force-controlled gravitational loading on the T-12 surface, the second will be the microgravity model that will have displacement-controlled loading on the T-12 surface that will stretch the spine to a length equal to its initial length plus 110% of thickness of all the IVDs to simulate stretching caused by microgravity, and the third will be the fetal tuck position model that will be run under the same conditions as the microgravity model, but with an additional step afterwards that will include force-controlled loading on the T-12 vertebra moving it in the anterior direction to simulate the fetal tuck position. All models will have the bottom nodes of the S1 vertebra fixed in place as a boundary condition. The gravitational model will have a 400N compressive force (negative z

direction) applied to the top nodes of the T12 vertebra. 400N is representative of the load on the lumbar spine in normal gravity.

The whole spine is stretched 110% of the combined IVD thickness due to the inherent difficulty of stretching every IVD individually. Stretching each IVD in a displacement-controlled manner would change the configuration of the whole model in a manner that would affect the stretching of the other IVDs. The IVDs are also the most likely to be affected by the stretch due to their comparative softness compared to the vertebrae. The model will be stretched in the vertically oriented direction (y-direction with respect to the model, superior with respect to the body). The thickness of each disc in the model is as follows, in mm:

T12-L1	L1-L2	L2-L3	L3-L4	L4-L5	L5-S1
7.08196	8.01240	9.15832	9.50928	13.6659	13.9073

Table 2 - The thickness of each IVD in the computational model.

for a total of 61.33516 mm. 10% of that value is 6.133516 mm, which is the amount that the T12 vertebral surface will be translated in the z-direction. The fetal tuck model will have a 10.5 kN spine flexion step after the microgravity step to represent the forward bend in the spine that occurs during the fetal tuck.

The stresses and strains on the facet joint membranes will be collected from the whole membrane, averaged, and compared between the gravity model and the microgravity model, and between the fetal tuck model and the microgravity model.

3.4 Results

Maximum principal strains were consistently higher for the gravity model over the microgravity model. The differences were greatest in the center portion of the model at the L2-L3 and the L3-L4 facet joints. Differences between the left and right facets of the pairs were negligible. The same phenomena can be observed for the maximum principal stress. The von Mises stresses were generally higher in the gravity simulation with exceptions at the T12-L1 facet joint where the values were close and the L5-S1 facet joint where the microgravity model had higher von Mises stress.

The data comparing the microgravity model to the fetal tuck position model followed similar patterns for all 3 measured metrics; Principal Strain, Principal Stress, and von Mises stress all were greater in the Fetal Tuck model compared to the Microgravity model for the T12-L1, L1-L2, and L5-S1 facet joints, most substantially so in the T12-L1 facet joint. The values for all 3 metrics at the other facet joints (L2-L3, L3-L4, and L4-L5) were all very similar.

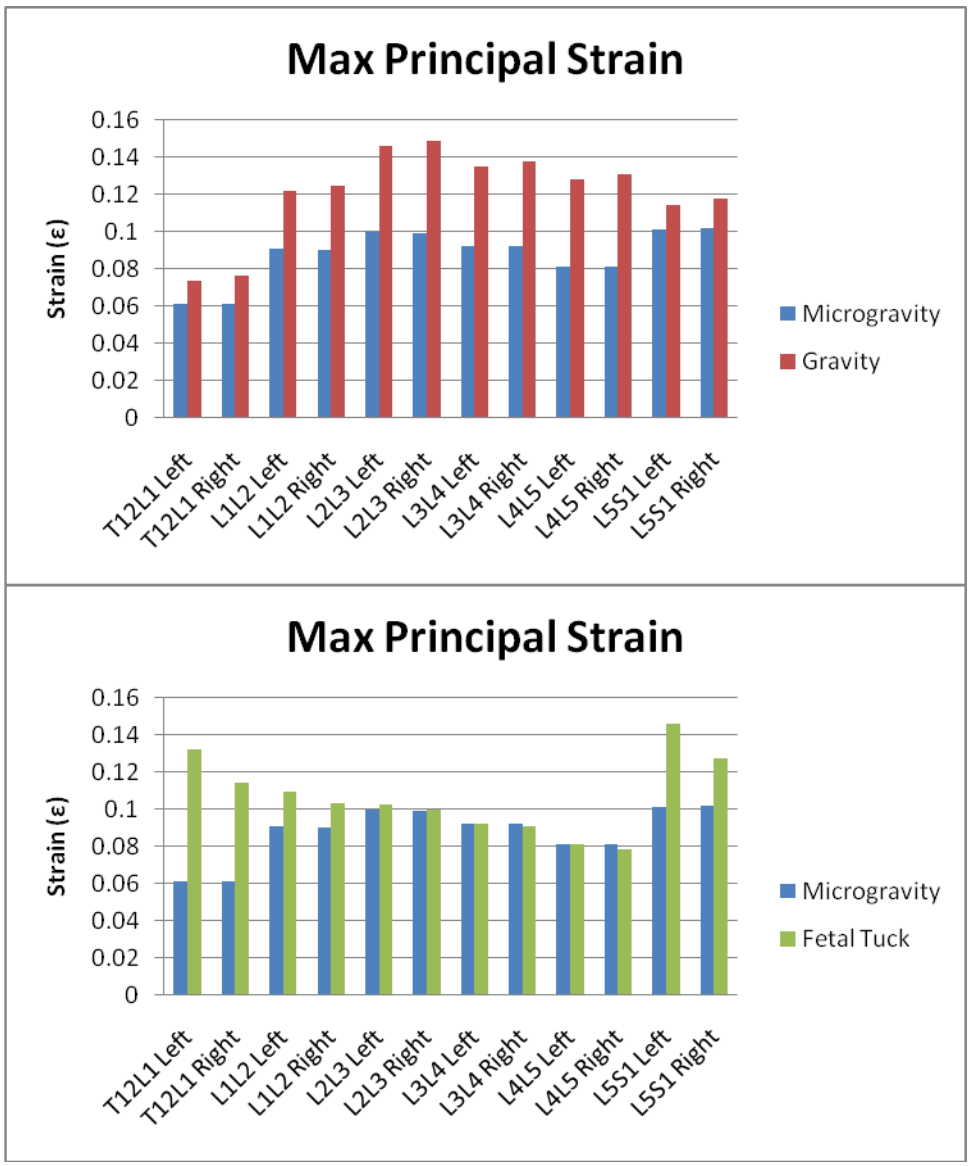

Figure 12 - Comparison of maximum principal strain between the micogravity and gravity and microgravity and fetal tuck models.

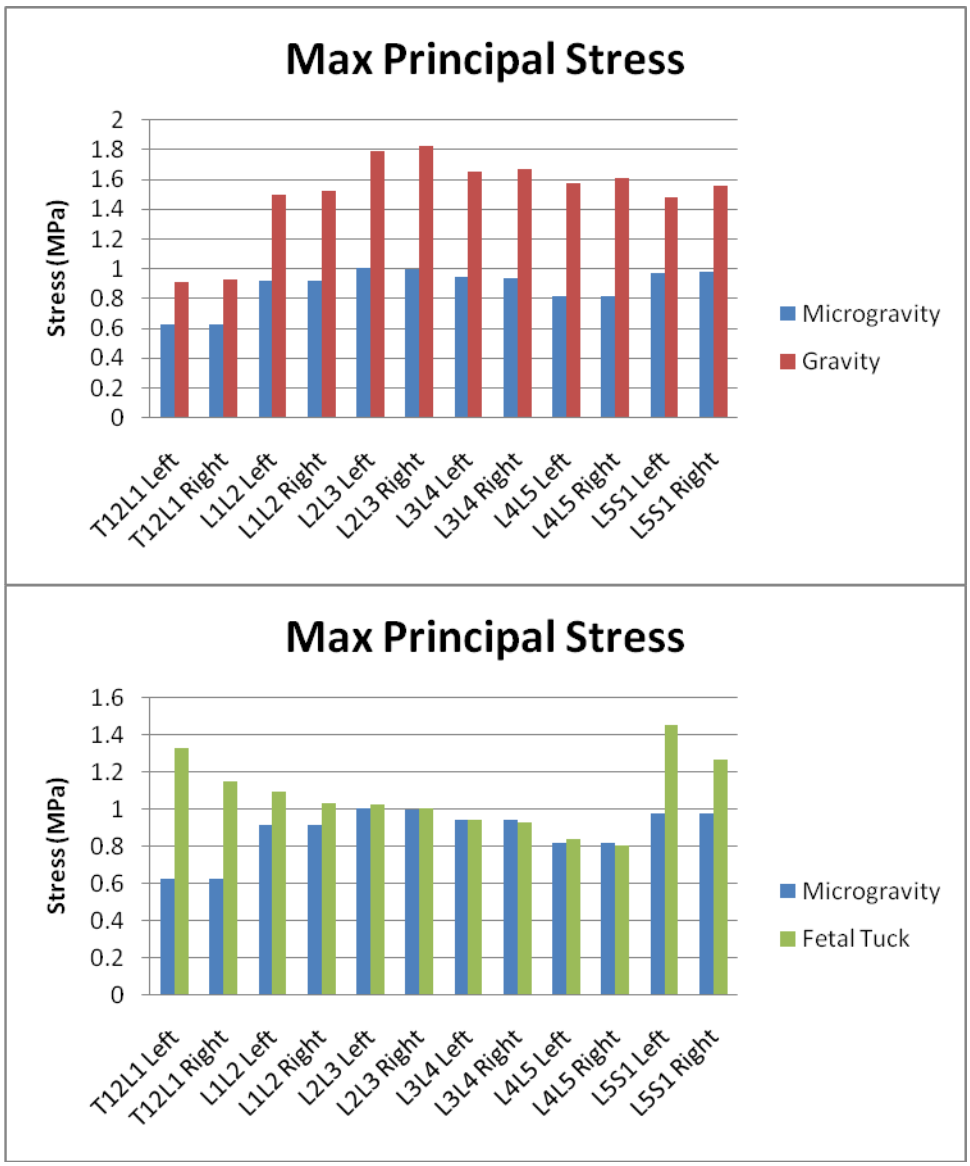

Figure 13 - Comparison of maximum principal stress between the micogravity and gravity and microgravity and fetal tuck models.

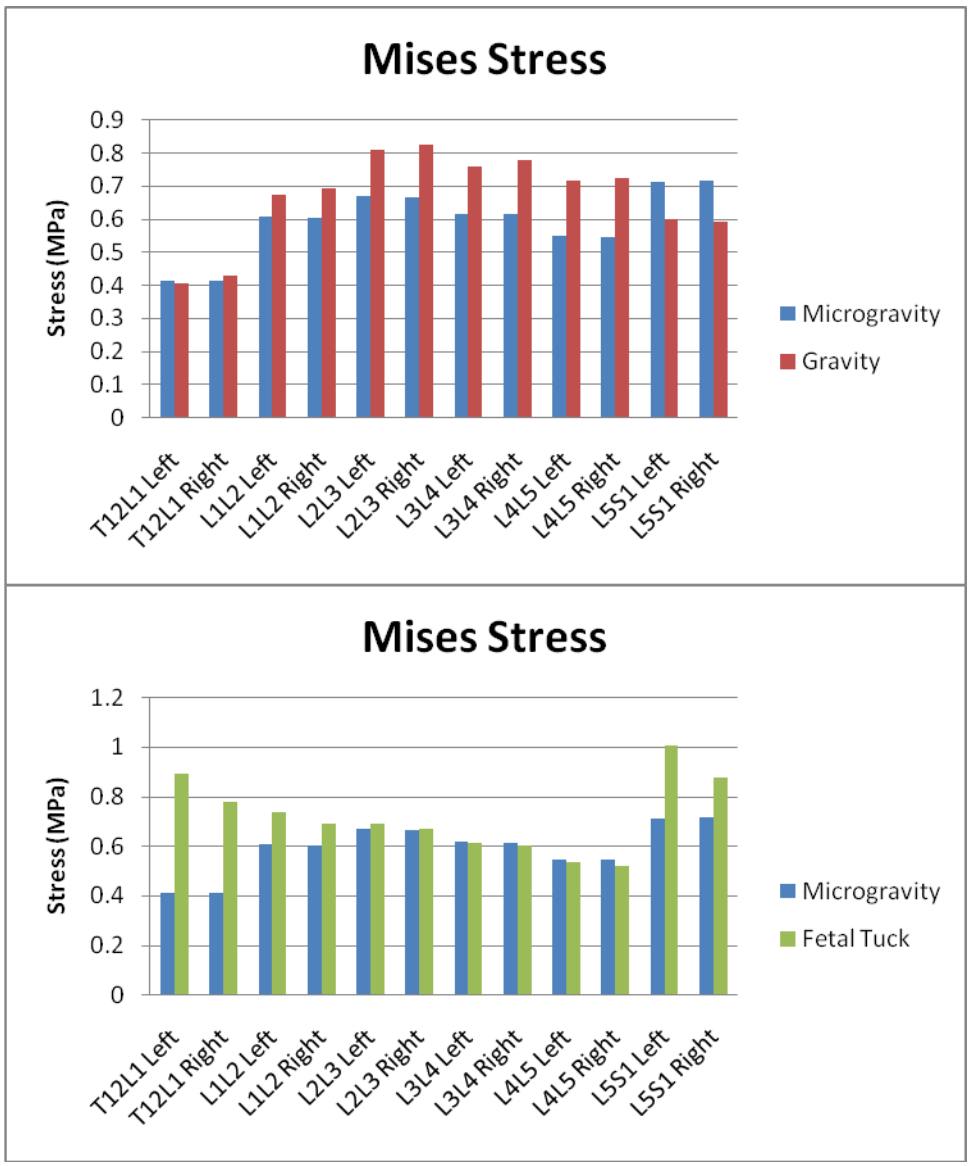

Figure 14 - Comparison of von Mises stress between the micogravity and gravity and microgravity and fetal tuck models.

3.5 Discussion

Prolonged exposure to an environment of microgravity is known to cause elongation of the spine. This is thought to be cause by the uptake of water into the nucleus pulposus of the intervertebral disc, which in an environment with gravity is squeezed out of the nucleus due to gravitational forces during diurnal activity when humans are upright. In this study, a simulation of a microgravity environment was applied to a computational model of the spine by elongating the spine via displacement control. The stresses and strains of the facets that occurred as a result of this were compared to a similar model exposed to gravitational forces and a microgravity model that applied a force to the spine similar in nature to curling into the fetal tuck position which has been known to alleviate low back pain in the microgravity setting. This was done in order to provide support to the theory that the facets do not have a role in low back pain due to microgravity. The data, by showing that in general the facet joints of the spine in microgravity have less stress and strain applied to them, supports that theory.

Stresses and strains in the principal directions were always greater in normal gravity than the corresponding stresses and strains in the microgravity model. During the space flight, the lesser load shows that there is no chance that the nocireceptors present on healthy facet membranes would be triggered. This has some interesting implications, however: although the normal spinal curvature is disrupted the facets do not take on more load. Less load on the facets also means that they play less of a role in stabilizing the spine. This could be a contributing factor to the low back pain some

astronauts suffer after a space flight. In addition, the lower loads experienced by the facets could cause the bone in the facets to remodel according to Wolff's Law to be weaker. Most bones do so during periods of microgravity, but the resulting facet joints may not be able to take loads once back in a gravitational environment.

The comparison between the microgravity and the fetal tuck models show that facet membranes are most likely not the cause of the pain relief due to stretching into the fetal tuck position. For all but 2 pairs of facets, the principal stress, principal strain, and von Mises stress values were comparable between the microgravity and fetal tuck models. The T12L1 facet membranes and L5S1 facet membranes were both greater in the fetal tuck model than the microgravity model. The lack of many differences between facet membrane stresses and strains supports the theory that facet membrane stretch is not the cause of pain relief due to the fetal tuck position. In addition, the stretches that generally result in pain relief often involve some sort of spinal twisting in the same way that SM is practiced.

This brings up an interesting question: whether pain relief via facet joints can even occur in microgravity. Microgravity causes standing fluids to act differently than when under gravity: they tend to organize into small bubbles and spread out in their container. If the synovial fluid acts in a similar manner, cavitation may not be possible. There have been no documented studies as to whether cavitation of any joints can occur in microgravity. It would be interesting to observe the action of synovial fluid of joints in microgravity to see if it acts as other standing fluids do in microgravity.

The biggest limitation of this study is the way in which the bulging fluid nucleus was modeled. In the human body, the bulging nucleus is caused by the nucleus being filled past the physiological normal amounts of fluid. This would technically mean that the disc is more massive than it normally is. To technically model this in an FE model would mean to completely remodel the nucleus to have larger dimensions. This would cause every other part of the model to be remodeled as a result, so the axial stretching was the pragmatic solution. Stretching each disc individually was another option, but would not be possible as a displacement controlled method due to the cascading movements to the model that would occur due to displacement controlled movement.

Overall, this study supports the theory that the facets do not play any role in LBP in microgravity. The generally lower strains on the facet membranes in microgravity than in gravity are the key data that supports this. In addition, the data shows that the facets do not play in a role in relief of LBP in microgravity. Facet membrane strains are mostly comparable between the fetal tuck and microgravity models. There is no reason why stretch-activated membrane proteins would be triggered by the fetal tuck position.

4. Degenerative Disc Disease and its Effect on FJC Membranes at and Around the Degenerated Disc

4.1 Background

An IVD is considered degenerated when it loses water and proteoglycan content and becomes stiffer as a result. Though etiology of IVD degeneration mechanics is not well defined; degeneration has traditionally been attributed to aging and excessive physical loading on the spine [38]. Other factors that are believed to contribute to degeneration, its progression, and the time of its onset include genetic factors, loss of nutrient flow to the disc, and lifestyle factors such as smoking and occupational conditions. An IVD has no blood flow through it, the closest blood vessel being 8mm away from it; it receives nutrition via diffusion over the vertebral endplates. This nutritional flow can be disrupted due to endplate calcification and other factors such as smoking and age [39].

Disc degeneration onset is earlier in men, where it first appears in their 20s, than women where it first appears in their 30s. However, by the age of 60 degeneration of at least one IVD can be detected in nearly all people [39]. Lumbar discs, specifically the L4-L5, L4-L5, and L5-S1 discs, are both the first discs to degenerate and the discs that most commonly degenerate. Radiographic symptoms that are indicative of degenerative disc disease (DDD) are the presence of osteophytes (bone spurs that form at joints), sclerosis of the end plates, and narrowing of the disc space. However, detection of DDD of a lumbar disc does not necessarily mean that it is the cause of low back pain. Most degenerated discs are asymptomatic: 34% of people ages 20-39 and

93% of people ages 60-80 without low back pain have a degenerated disc that can be detected via radiography [10].

In a normal IVD the annulus is composed of concentric collagen fibers embedded in a proteoglycan matrix. As a result the structure can support multidirectional loads in tension, compression, shear, bending, and torsion. When the annulus degenerates, the hydrophilic proteoglycan content is decreased, this also decreases the water content in the annulus. Collagen content in the annulus is increased as well. The resulting mechanical properties of the degenerated disc are increased stiffness in compression and shear [40].

The changes in a degenerated nucleus pulposus is even more pronounced, with the nucleus shifting from fluid-like behavior to solid-like behavior. The loss of aggrecan proteoglycans and chondroitin Glycosaminoglycans (GAGs) coupled with the buildup of keratin GAGs and collagen I in the nucleus is the reason for this. This causes the nucleus to be unable to hold water and ultimately lose its ability to hold hydrostatic sress, resulting in load shifting to the annulus, decreased disc height, and sometimes a bulging disc [39].

There are a number of theories as to why most cases of DDD are asymptomatic while others cause LBP. One theory is that the degenerated disc causes abnormal motion in the disc which set of mechanical stimuli in the nocireceptors that innervate the annulus. This is known as discogenic pain. It is also theorized that degeneration of the disc causes granulation tissue to form in the nucleus pulposus. This causes mast cells to migrate to the nucleus, which in turn cause further degradation via fibrocartilage

production, neovascularization, and nucleus tissue degradation as well as encouraging innervations of the nucleus [39].

Another possible cause for pain due to DDD is the shift of load to the facet joint capsule. While stiffer, a degenerated disc loses the ability to bear loads due to the loss of proteoglycans and water content in the nucleus, which in turn causes a shift of load bearing to the facet joints. The FJCs normally carry 3-25% of the total load on the spine during extension, compression, and rotation [41]; an increase past this amount can cause malignant changes in the facet joint such as cartilage wear and bone spurs formation.

4.2 Hypothesis

The objective of this study is to determine whether degenerated IVDs cause any changes in the loads experienced by FJCs; not only the FJCs that are in the same gap as the degenerated FJCs, but also the FJCs in the other intervertebral gaps. The hypothesis for this study is that FJCs in the same intervertebral gap of a degenerated disc will have altered load while those not in the same gap will not. The specific aim of this study is to use the finite element model of the t12-s1 spine in physiologic loading conditions to observe whether or not loading is on the facet joints is altered, and if so, which facet joints are affected.

4.3 Methods

4.3.1 Model Development

The simulations for this study will use the previously described T12-S1 spine model with detailed, linear FJCs and modified versions of the same model. To review, the model contains the bony parts of the spine as well as the nucleus and annulus of the IVD modeled as linear elastic materials with the ligaments modeled as hypoelastic materials. The facets are modeled as linear elastic materials with an elastic modulus chosen from the best fit from specific aim 1, connected to the model proper with tie commands, and connected at the joint by space elements with friction properties to simulate the bearing of the FJC's synovial joint. All values are taken from previous literature. The modified models will each have a degenerated disc at a different location, taken from the IVDs that are most commonly found to be degenerated: L3-L4, L4-L5, and L5-S1; including the control model there will be 4 models. The degenerated discs will have different materials properties from the healthy discs: the Young's modulus of the Ground substance of the healthy annulus is E=4.2 MPa with a Poisson's ratio of 0.45 while the Young's modulus of the degenerated annulus is E=12.29 with a Poisson's ratio of 0.35. Likewise, the modulus of the nucleus is E=1.0 MPa for a healthy nucleus and 1.66 for a degenerated nucleus, with a Poisson's ratio of 0.49 (denotes incompressibility). The embedded fibers in annulus will not be changed.

4.3.2 Loading Conditions

All models will be tested under 3 sets of loading and boundary conditions based on physiologic motions: 10.5 kN anterior flexion, 10.5 kN lateral deflection, and 10.5 kN CCW rotation. In total there will be 8 models run. The loads will all be applied to the central node on the top surface of the T12 vertebra. The bottom of the S1 vertebra will be fixed in all 6 dimensions. Values for stresses and strains on the facet membranes and the IVDs will be collected: Maximum principle strain, Maximum principle stress, and Von Mises stress. Stress and strain values will be compared between the healthy annulus of the IVDs and the degenerated annulus of the IVDs for changes. Stress and strain values for all facet membranes in each model will be compared for changes between the healthy model and the degenerated model. Stress and strain values will be obtained from the whole tissue modeled and averaged.

4.4 Results

The greatest differences between the control and experimental groups observed for principal stress, principal strain, and von Mises stress were always at the spot of the degenerated disc present in the model. In the CCW rotation models, no facets other than the ones adjacent to the degenerated disc were affected in the L3L4 degenerate and L4L5 degenerate models, but in the L5S1 degenerate model all other facets were affected to some degree. In the flexion model, the only facets other than the set at the same intervertebral gap that had the degenerated disc were the ones in the intervertebral gap adjacent to the degenerated disc: L2L3 and L4L5 for the the degenerated L3L4 model, L3L4 and L5S1 for the degenerated L4L5 model, and L4L5 for the degenerated L5S1 model. The same phenomenon was observed in the CCW rotation models. All three loading cases exhibited asymmetric loading favoring the right facets of each pair.

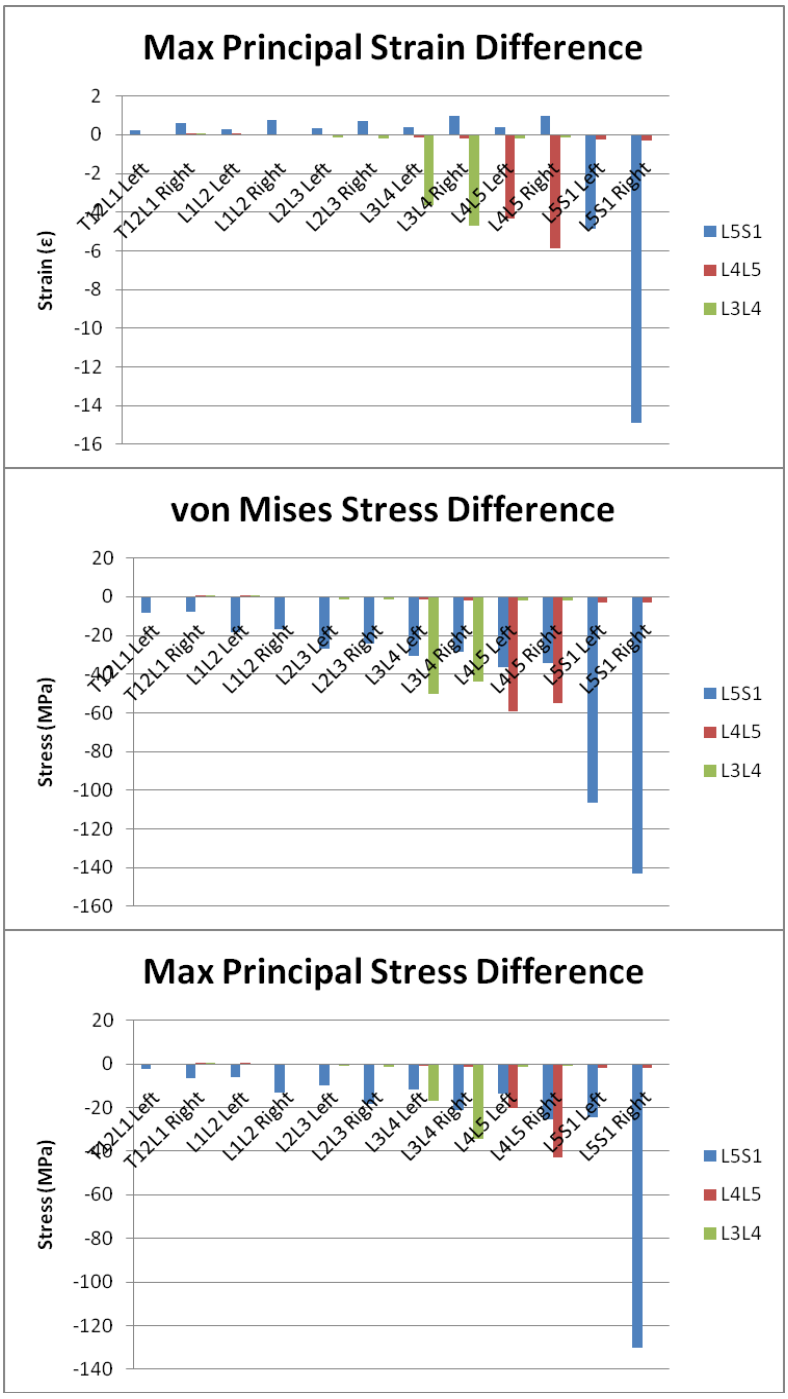

Figure 15 - Data for lateral bending of the spine. These graphs show the difference between the values recorded for the degenerated models and the non-degenerated control model. The legend denotes which disc was degenerated in the model

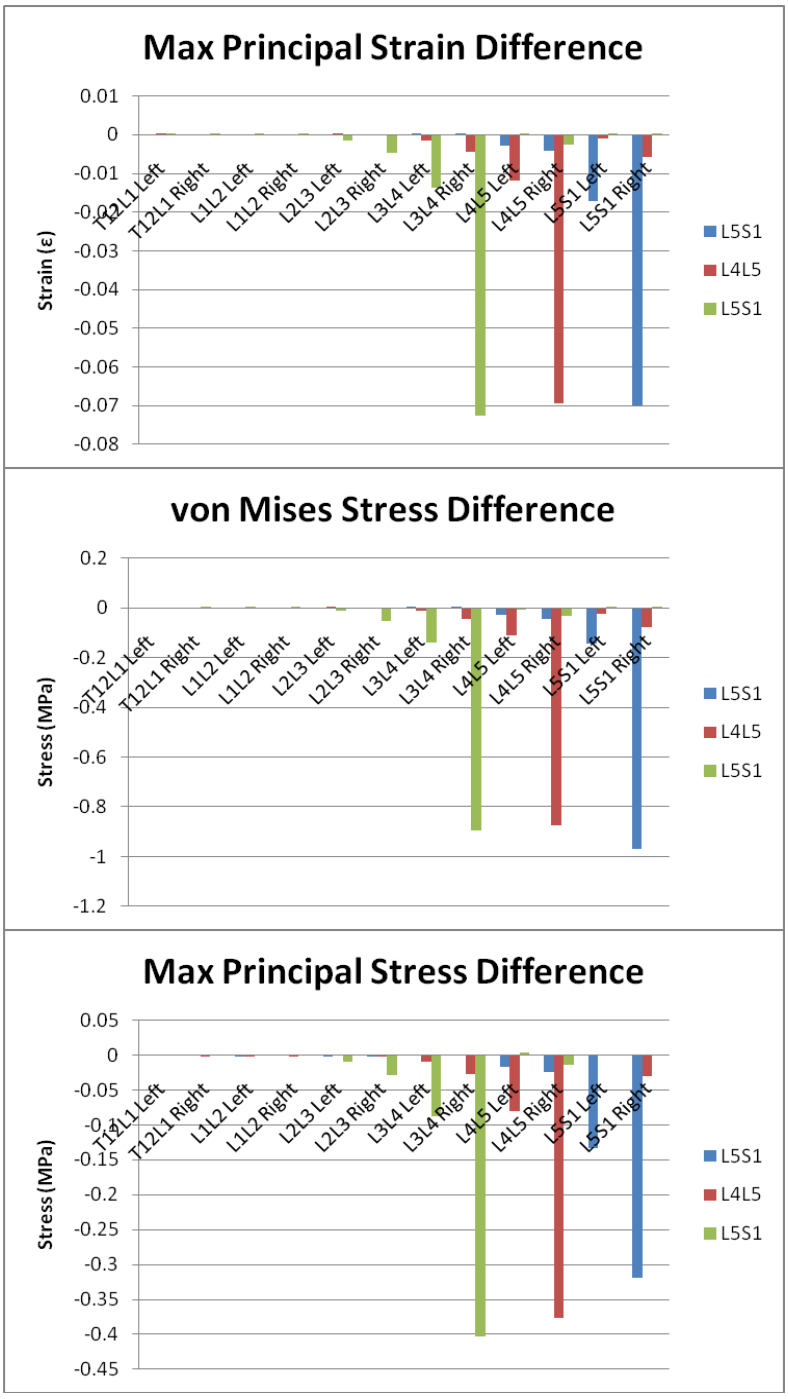

Figure 16 - Data for anterior flexion of the spine. These graphs show the difference between the values recorded for the degenerated models and the non-degenerated control model. The legend denotes which disc was degenerated in the model

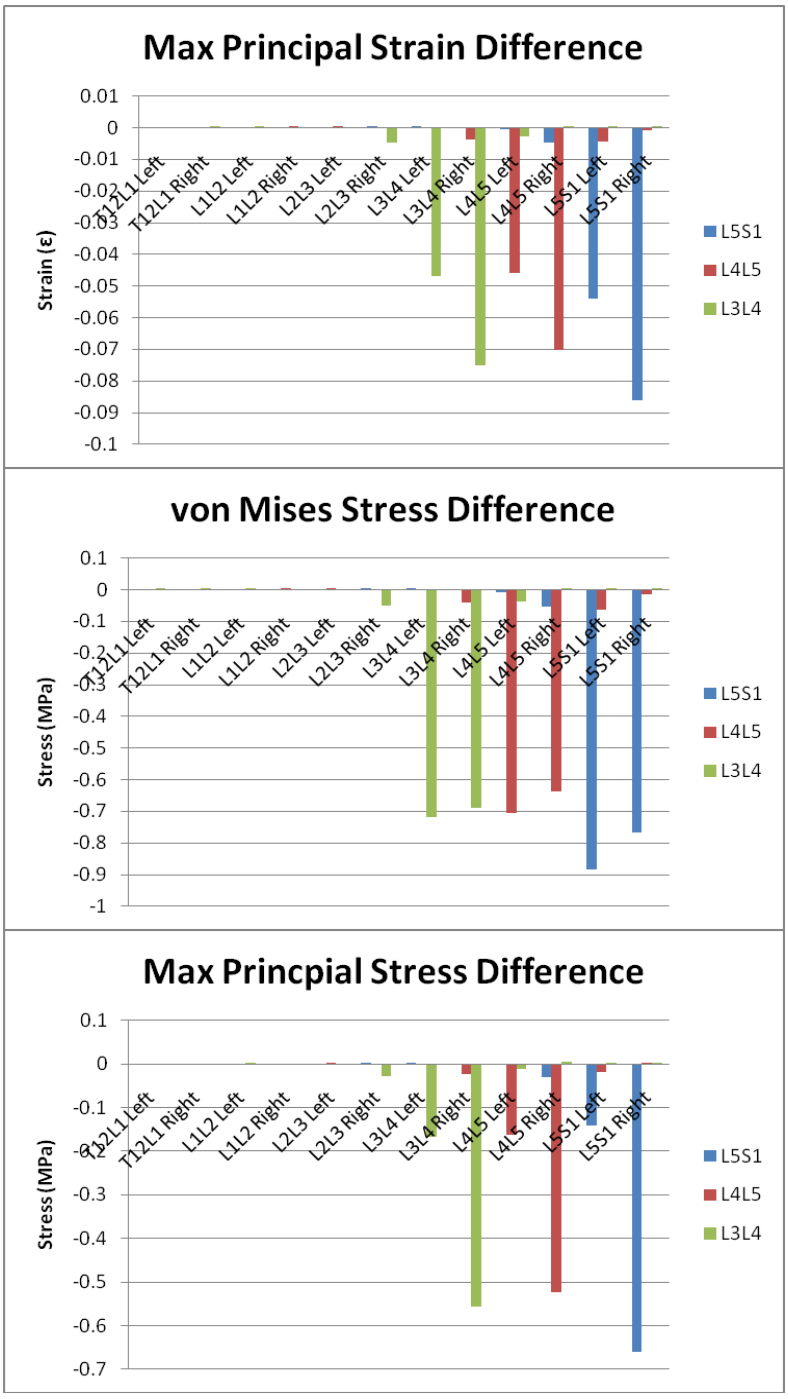

Figure 17 - Data for CCW rotation of the spine. These graphs show the difference between the values recorded for the degenerated models and the non-degenerated control model. The legend denotes which disc was degenerated in the model

4.5 Discussion

Degenerated intervertebral discs are a known cause of low back pain. However, the actual mechanism of pain is unknown, but nocireceptors on the facet membrane are thought to be a contributing factor to LBP. Many studies have examined the effect of degenerated discs on the facet joint in the same intervertebral gap as the disc but few have studied the effect on facets at different gaps. This study shows that the facets at intervertebral gaps adjacent to the gap containing the disc are affected by the degenerated disc. This leads to implications as to the progression of DDD to other IVDs.

The first part of the data that stands out is that the difference between the stresses and strains of the non-degenerative control groups and degenerative experimental groups are all negative, denoting that the stresses and strains measured for the degenerative groups was less than the control groups. Despite the theory that high facet joint strains may be the cause of back pain from degenerative discs, this lines up with previous studies using similar models. DDD is often accompanied by degeneration of other structures in spine, including the facets. In addition, the degeneration may also cause neo-innervation of both the discs and the facets, which would then transmit the pain stimulus. Therefore, the lesser stresses and strains in this model is to be expected.

The anterior flexion data also has an odd aspect. Flexion should have a symmetrical response, but the strains favor the right facet. Indeed, ABAQUS Viewer shows the model deflecting to the right. This was unexpected, especially seeing similar loading conditions were used for the fetal tuck position in specific aim 2 and those

results were symmetric. For the purpose of this study, the anterior flexion data is inconclusive and must be discarded because of the unexpected response, as the asymetric response may be a flaw of the model.

The asymetric response for maximum principal stress and strain is to be expected from the CCW rotation and lateral bending studies. The data from the lateral bending condition indicates that degenerated discs do not affect other joints in rotation. Both the L3L4 and L4L5 degenerated models do not show substantial difference between the stresses and strains of the facet membranes other than those of the L3L4 and L4L5 membranes. Although the L5S1 degenerated model caused differences in all of the facets in model, this is likely due to the proximity of the L5S1 IVD to the boundary condition at the bottom of the model: the S1 vertebrae is not as fully defined as the other vertebrae. Thus, the boundary condition could almost be considered to be on the IVD itself, which would cause data to be skewed.

However, the CCW rotation condition does show that the degenerated discs affect adjacent facets: the L5S1 degenerated disc causes change in the L4L5 facet membrane stresses and strains, the L4L5 degenerated disc causes change in the L3L4 and L5S1 facet membrane stresses and strains, and the L3L4 degenerated disc causes change in the L3L4 and L5S1 facet membrane stresses and strains. One of the follow-up effects of altered loads due to degenerated discs is further degeneration of the structures surrounding it. If a degenerated disc truly causes loading changes in other vertebral gaps, it could hasten the degeneration of the structures with altered loading. Something to consider for future studies would be to also examine the changes in

loading on the adjacent discs as well as the facets. Research should also be done on the location in which patients get degenerated discs subsequent to their first. The data suggests that those discs near the ones already degenerated should be the next to follow suit.

References

1. Thomson, O., L. Haig, and H. Mansfield, *The effects of high-velocity low-amplitude thrust manipulation and mobilisation techniques on pressure pain threshold in the lumbar spine.* 2009. **12**(2): p. 56-62.

2. Evans, D.W., *Mechanisms and effects of spinal high-velocity, low-amplitude thrust manipulation: Previous theories.* Journal of Manipulative and Physiological Therapeutics, 2002. **25**(4): p. 251-262.

3. Shiri, R., et al., *Incidence of nonspecific and radiating low back pain: followup of 24–39-year-old adults of the Young Finns Study.* Arthritis Care & Research, 2010. **62**(4): p. 455-459.

4. Griffith, L., E. , et al., *Low-back pain definitions in occupational studies were categorized for a meta-analysis using Delphi consensus methods.* Journal of clinical epidemiology, 2007. **60**(6): p. 625.e1-625.e23.

5. Luo, X.P., et al., *Estimates and Patterns of Direct Health Care Expenditures Among Individuals With Back Pain in the United States. [Miscellaneous].* Spine, 2004. **29**(1): p. 79-86.

6. Manchikanti, L.S., V; Falco, FJE; Cash, KA; Pampati, V., *Evaluation of Lumbar Facet Joint Nerve Blocks in the Management of Chronic Low Back Pain: Preliminary Report of a Randomized, Double-Blind Controlled Trial: Clinical Trial.* Pain Physician Journal, 2007. **10**(3): p. 425-440.

7. Guo, H.R., et al., *Back pain prevalence in US industry and estimates of lost workdays.* Am J Public Health, 1999. **89**(7): p. 1029-1035.

8. Manek, N.J. and A.J. MacGregor, *Epidemiology of back disorders: prevalence, risk factors, and prognosis.* Current Opinion in Rheumatology, 2005. **17**(2): p. 134-140.

9. Krismer, M. and M. van Tulder, *Low back pain (non-specific).* Best practice & research. Clinical rheumatology, 2007. **21**(1): p. 77-91.

10. Schizas, C.K., G; Kosmopoulos, V, *Disc Degeneration: Current Surgical Options.* European Cellls and Materials, 2010. **20**: p. 306-315.

11. Nau, W.H., et al., *Intradiscal Thermal Therapy Using Interstitial Ultrasound: An In Vivo Investigation in Ovine Cervical Spine.* Spine, 2007. **32**(5): p. 503-511 10.1097/01.brs.0000256905.39488.c7.

12. Nau, W.H.D., Chris J; Shu, Richard, *Feasibility of using interstitial ultrasound for intradiscal thermal therapy: a study in human cadaver lumbar discs.* Physics in Medicine and Biology, 2005. **50**(12): p. 2807.

13. Koes, B.W., et al., *The efficacy of back schools: A review of randomized clinical trials.* Journal of clinical epidemiology, 1994. **47**(8): p. 851-862.

14. Berman, B.M., et al., *Effectiveness of Acupuncture as Adjunctive Therapy in Osteoarthritis of the Knee.* Annals of Internal Medicine, 2004. **141**(12): p. 901-910.

15. Wolsko, P.M., et al., *Patterns and Perceptions of Care for Treatment of Back and Neck Pain: Results of a National Survey.* Spine, 2003. **28**(3): p. 292-297.

16. Curtis, P., *Spinal Manipulation: Does it work?* Occupational Medicine, 1988(3): p. 31-44.

17. Shekelle, P., et al., *Spinal manipulation for low-back pain.* Annals of Internal Medicine, 1992. **117**(7): p. 590-598.

18. Sandoz, R., *The significance of the manipulative crack and of other articular noises.* Annals of the Swiss Chiropractic Association, 1969(4): p. 47-68.

19. Hessel, B., et al., *Experimental measurement of the force exerted during spinal manipulation using the Thompson technique.* Journal of Manipulative and Physiological Therapeutics, 1990(13): p. 448-453.

20. Lisi, A.J., E.J. Holmes, and C. Ammendolia, *High-Velocity Low-Amplitude Spinal Manipulation for Symptomatic Lumbar Disk Disease: A Systematic Review of the Literature.* Journal of Manipulative and Physiological Therapeutics, 2005. **28**(6): p. 429-442.

21. Herzog, W., et al., *Cavitation sounds during spinal manipulative treatments.* Journal of Manipulative and Physiological Therapeutics, 1993(16): p. 523-526.

22. Mercer, S. and N. Bogduk, *Intra-articular inclusions of the cervical synovial joints.* British Journal of Rheumatology, 1993(32): p. 705-710.

23. Giles, L.G.F. and J.R. Taylor, *Human Zygapophyseal Joint Capsule and Synovial Fold Innervation.* Rheumatology, 1987. **26**(2): p. 93-98.

24. Bogduk, N. and G. Jull, *The Theoretical Pathology of Acute Locked Back: a Basis for Manipulative Therapy.* Manual Medicine, 1985(1): p. 78-82.

25. Pickar, J.G., *Neurophysiological effects of spinal manipulation.* The spine journal : official journal of the North American Spine Society, 2002. **2**(5): p. 357-371.

26. Unsworth, A., D. Dowson, and V. Wright, *A bioengineering study of cavitation in the metacarpophalangeal joint.* Annals of the Rheumatic Diseases, 1971(30): p. 348-358.

27. Burton, A., et al., *Lumbar spinal mobility and low back symptoms in patients treated with manipulation.* Journal of Spinal Disordorder, 1990(3): p. 262-268.

28. Johnston, S., M. Wear, and P. Hamm, *Increased Incidence of Herniated Nucleus Pulposus Among Astronauts and Other Selected Population.* Avaiation, Space, and Environmental Medicine, 1998. **69**(3): p. 220.

29. Mullane, M., *Riding Rockets: The Outrageous Tales of a Space Shuttle Astronaut*. 2006: Scribner.

30. Whalen, R., *Musculoskeletal adaptation to mechanical forces on Earth and in space.* Physiologist, 1993(36): p. S127-S130.

31. Brown, J., *Crew Height Measurements, the Apollo-Soyuz Test Project Medical Reports*, NASA, Editor. 1977, NASA: Washington, DC.

32. Kimura, S., G. Steinbach, and D. Watenpaugh, *Lumbar Spine Disc Heigh and Curvature Responses to an Axial Load Generated by a Compression Device Compatible with magnetic resonance imaging.* Spine, 2001. **26**(23): p. 2596-2600.

33. Hargens, A., *Interstitial osmotic pressure associated with donna equilibria*, in *Tissue fluid pressure and composition*. 1986, Williams and Wilkins: Baltimore. p. 77-85.

34. Sivans, S., C. Nedilinger-Wilke, and K. Wurtz, *Diurnal fluid expression and activity of intervertebral discs.* Biorheology, 2006. **43**(3-4): p. 283-291.

35. Sayson, J. and A. Hargens, *Pathophysiology of Low Back Pain during Exposure to Microgravity.* Avaiation, Space, and Environmental Medicine, 2008. **79**(4): p. 365-373.

36. Hargens, A., K. Hutchinson, and R. Ballard, *Intervertebral disc: loaded on Earth and unloaded in space, connective tissue biology, itegration, and reductionism*. Vol. 7. 1998, London: Portland Press Ltd.

37. Putcha, L., B. Berens, and T. Marshburn, *Pharmaceutical use by U.S. astronauts on space shuttle missions.* Avaiation, Space, and Environmental Medicine, 1990. **70**(7): p. 705-708.

38. Cheung, K.M.C., *The relationship between disc degeneration, low back pain, and human pain genetics.* The spine journal : official journal of the North American Spine Society, 2010. **10**(11): p. 958-960.

39. Choi, Y.-S., *Pathophysiology of Degenerative Disc Disease.* Asian Spine J, 2009. **3**(1): p. 39-44.

40. O'Connell, G.D., H.L. Guerin, and D.M. Elliott, *Theoretical and Uniaxial Experimental Evaluation of Human Annulus Fibrosus Degeneration.* Journal of Biomechanical Engineering, 2009. **131**(11): p. 111007-7.

41. Yang, K. and A. King, *Mechanism of facet load transmission as a hypothesis for low-back pain.* Spine, 1984(9): p. 557-565.